

Microwave radiation at criticality in a hybrid Josephson array

Kristen W. Léonard,^{1,*} Anton V. Bubis,^{1,*} Melissa Mikalsen,² William F. Schiela,² Bassel H. Elfeky,² Duc Phan,¹ Javad Shabani,² and Andrew P. Higginbotham^{3,1,†}

¹*Institute of Science and Technology Austria, Am Campus 1, Klosterneuburg, 3400, Austria*

²*Department of Physics, Center for Quantum Phenomena,*

New York University, New York, NY, 10003, USA

³*James Franck Institute and Department of Physics,*

University of Chicago, 929 E 57th St, Chicago, Illinois 60637, USA

Anomalous metallic behavior is ubiquitously observed near superconductor-insulator quantum critical points and, if persistent to zero temperature, poses a challenge to current theories of metals [1]. One explanation for this behavior could be incomplete thermal equilibrium between the sample and the cryostat. However, despite decades of study, the actual temperature of an anomalous metallic sample has not been measured. We therefore introduce a new experimental probe by measuring microwave radiation emitted from the anomalous metal, using a two-dimensional array of superconductor-semiconductor hybrid Josephson junctions as a model system. The total emitted radiation exceeds the limits of thermodynamic equilibrium, but is well described by an elevated sample temperature. This extracted sample temperature matches the onset of anomalous metallic behavior. Additionally, we discover scaling behavior of radiative noise in the presence of an applied bias. Elements of our noise-scaling observations were predicted based on nonlinear critical field theories [2, 3] and gauge-gravity duality [4]. This work shows that, in a prominent model system, anomalous metallic behavior is a non-equilibrium effect, and opens a new frontier in the study of universal, non-equilibrium phenomena near quantum criticality.

A broad regime of low-temperature resistance saturation is commonly observed in proximity to the superconductor-insulator transition (SIT) [5–12]. This anomalous metallic regime occurs in a strikingly wide array of platforms and materials, including the Josephson-junction arrays under study in this work, and has been discussed as a challenge to the theoretical understanding of metallic behavior at $T = 0$ [1]. On the other hand, in several cases it has been experimentally shown that increased filtering restored a direct superconductor-insulator transition with no intervening metal, indicating that the anomalous metallic regime occurred due to a lack of thermalization [13, 14]. Currently, it is unclear if anomalous metallic behavior is caused by a lack of thermal equilibrium with the cryostat. We will show that this question can be resolved by measuring radiation emitted in the anomalous metallic regime.

Fundamentally, the non-equilibrium behavior of superconductor-insulator systems has been a subject of great theoretical interest. Owing to the presence of integrability in the limit of high energy density, arrays of Josephson junctions theoretically exhibit slow thermalization in the classical case [15, 16]. In the quantum case, many-body localized and multi-fractal metallic phases are predicted [17, 18]. Near the superconductor-insulator transition, analyses based on critical field theories [2, 3] and gauge-gravity duality [4] have predicted that non-equilibrium noise is described by an effective temperature whose scaling with applied bias is controlled only by the dynamical critical exponent. Testing

these predictions requires an experimental probe of the non-equilibrium behavior, moving beyond the traditional transport probes of superconductor-insulator physics.

Here, we answer this challenge by measuring the microwave radiation emitted by an array of Josephson junctions proximal to the superconductor-insulator transition. Focusing on a two-dimensional array of superconductor/semiconductor hybrid Josephson junctions as a tunable model system [10], we find excess radiation coincident with the onset of resistance saturation. Adapting methodology from the calibration of microwave radiometers [19], quantum-limited amplifiers [20], and axion haloscopes [21], we convert measured microwave noise power to an equivalent sample temperature. This extracted temperature is found to be compatible with the sample falling out of equilibrium with the cryostat at the onset of resistance saturation.

Motivated by predictions of universal scaling behavior near quantum critical points [3, 4], we additionally use our experimental apparatus to probe non-equilibrium radiation in the presence of an applied bias. We discover that the effective non-equilibrium sample temperature exhibits scaling as a function of current, qualitatively reproducing theoretically anticipated behavior. Quantitatively however, our results deviate from the predictions in several significant ways, leaving open space for re-interpretation of theoretical estimates. With our apparatus we thereby demonstrate a new experimental path for studying the non-equilibrium response of quantum critical systems.

The key technical innovation of our experiment is to connect an anomalous metallic system to a microwave readout chain (Fig. 1a). Coupling capacitors allow microwave radiation (black arrow) to be efficiently col-

* Equal contribution

† ahigginbotham@uchicago.edu

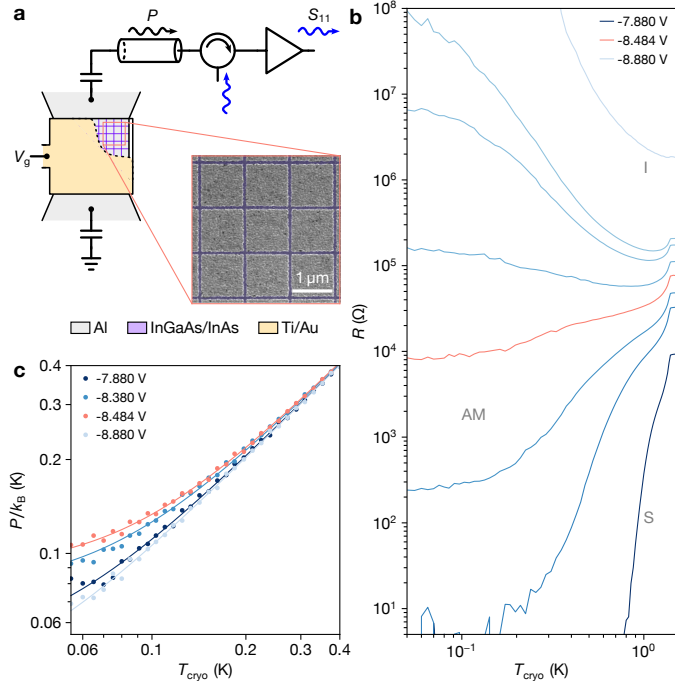


FIG. 1. **a**, Schematic of the device showing the Al/InAs Josephson junction array capacitively coupled to a microwave readout chain, with a top-gate to tune carrier density in the InAs two dimensional electron gas. A circulator and filtering (not pictured) prevents back-action noise from disrupting the anomalous metallic state, and allows it to be probed with a weak microwave tone. Standard quasi-four-probe transport measurement omitted from schematic for clarity. Scanning electron micrograph of the Al islands is shown in the inset. **b**, Measured resistance R versus cryostat temperature T_{cryo} at different top-gate voltages (indicated by colors). **c**, Measured radiation P as a function of T_{cryo} for selected top-gate voltages. The most excess radiation is observed at a top-gate voltage of -8.484 V, shown in panels **b** and **c** in salmon color. Solid lines are a model for an effective saturation radiation, P_{sat} , determined via best fit to each curve. The values of P_{sat}/k_B for each top-gate voltage are -7.88 V: 49 mK; -8.38 V: 76 mK; -8.484 V: 89 mK; -8.88 V: 37 mK.

lected and measured, while a circulator and filtering prevent back-action effects on the fragile anomalous metallic state. As a flexible model system for superconducting, insulating, and anomalous metallic regimes, we study a two-dimensional array of superconductor/semiconductor Al/InAs Josephson junctions [22, 23]. Josephson junctions are formed from the two-dimensional electron gas situated in the 4 nm-thick InAs quantum well spaced 10 nm below the Al layer. Measurements of two devices (S1, S2) are presented, with all reported measurements from device S1 unless otherwise indicated. Device S1 consists of a 40 wide x 100 long array of Al squares with periodicity 1.15 μm , spaced by 0.08 μm (Fig. 1a), and device S2 has the same proportions as S1 but the opposite aspect ratio: a 100 wide x 40 long array of Al islands. In

both devices a 50 nm-thick Al top-gate is deposited over a 60 nm Al_2O_3 dielectric layer covering the entire array. The measurements were carried out in a dilution refrigerator with a base temperature of 50 mK. Noise measurements were carried out in a 10 MHz band around 1.42 GHz, and uncalibrated microwave reflection (S_{11} , blue arrows in Fig. 1a) was measured and averaged in the same frequency band. Microwave spectroscopy measurements were carried out in a wider band of 1.15–1.75 GHz defined by the cryogenic circulator. Standard quasi-four-probe resistance measurements were performed with an AC bias of 5 μV over the lines in the cryostat and the sample.

It is useful to categorize sample behavior based on the dependence of measured resistance on cryostat temperature. For modest top-gate voltages, resistance decreases sharply with temperature, falling below the measurement threshold of our equipment and displaying a supercurrent, indicating a superconducting state (S, Fig. 1b). In contrast, for more negative top-gate voltages resistance increases sharply with temperature, indicating insulating behavior (I, Fig. 1b). At intermediate top-gate voltages, there is an initial drop in resistance as the cryostat temperature is lowered, followed by a low-temperature saturation to a small but nonzero value (AM, Fig. 1b). This low-temperature saturation near the critical point of the SIT is the hallmark behavior of the anomalous metal. The observed superconducting, anomalous metallic, and insulating regimes qualitatively reproduce previous work on the same platform [10]. We have observed varying degrees of low-temperature saturation depending on sample and setup configurations (see Supplement). We have also verified that resistance saturation occurs in samples that are not connected to microwave circuitry.

The simultaneously measured microwave power spectral density P on the input of the cryogenic amplifier depends linearly on cryostat temperature for high T_{cryo} , as expected based on the thermal equilibrium relation $P = k_B T_{\text{cryo}}$ (Fig. 1c). At lower temperatures P saturates, indicating non-equilibrium behavior. The data are well described by a phenomenological equation with a gate voltage dependent saturation power P_{sat} , according to $P^2 = k_B^2 T_{\text{cryo}}^2 + P_{\text{sat}}^2$. The saturation power is largest when the sample is tuned near the critical resistance of the superconductor-insulator transition. Studying the excess, non-equilibrium noise near the SIT is the central focus of this work. In what follows, we demonstrate the origin of the excess noise and show how to interpret it in terms of an effective sample temperature.

A more detailed understanding of excess noise at the superconductor-insulator transition can be obtained by studying the system's evolution with gate voltage at fixed cryostat temperature. Measured device resistance increases with decreasing gate voltage (Fig. 2a). At lower temperatures, the increase in resistance becomes more dramatic, with isothermal resistance curves crossing at a resistance separatrix of approximately 60 $\text{k}\Omega$, corresponding to a critical sheet resistance of 24 $\text{k}\Omega$. For com-

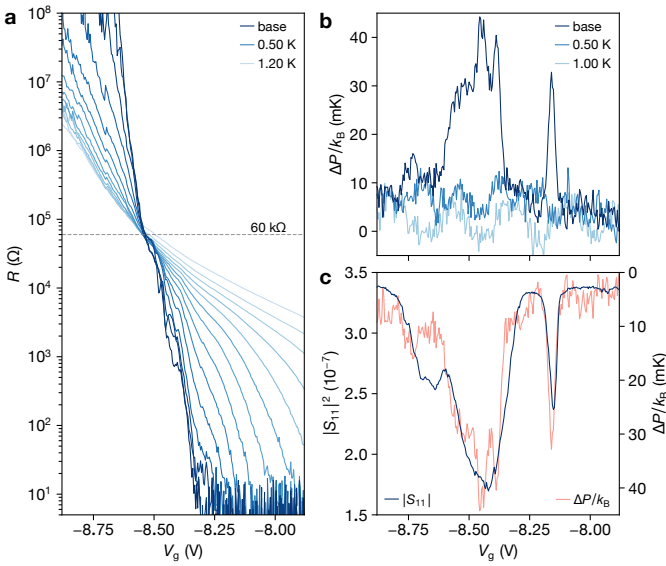


FIG. 2. **a**, Measured resistance R as a function of top-gate voltage V_g for different cryostat temperatures (indicated by colors). Resistance curves cross at the critical point indicated by the separatrix with resistance ≈ 60 kΩ (indicated). **b**, Excess noise ΔP versus V_g for different cryostat temperatures. ΔP is defined as the measured microwave power spectral density P minus the value measured deep in the superconducting phase, at the highest gate voltage in each trace; it represents the noise in excess of thermal-equilibrium expectations. Large excess noise is observed at low temperature (darkest blue trace). **c**, Reflection coefficient $|S_{11}|^2$ (left axis) and ΔP at 10 mK from panel **b** (right axis) versus V_g . Excess noise is strongly negatively correlated with $|S_{11}|^2$.

parison, the (2+1)D XY model has a critical resistance of 22.6 kΩ in the clean limit [24], and a smaller value of 12.9 kΩ in the disordered case [25]. Experimentally, critical points in other anomalous metallic systems have been reported at or near $h/4e^2 = 6.5$ kΩ [10, 26].

For elevated cryostat temperature, negligible excess noise is observed at all gate voltages, a signature expected for a system in equilibrium (Fig. 2b). However, at base temperature significant excess noise is observed, peaked slightly on the superconducting side of the SIT. Elevated radiation levels are observed throughout the anomalous metallic regime identified in Fig. 1b. These observations are compatible with the temperature-dependent noise study in Fig. 1b, and together indicate at the very least a broad region of non-equilibrium behavior surrounding the superconductor-insulator transition. Additionally, a solitary, sharp spike in excess noise is observed at -8.16 V, well within the ostensibly superconducting region.

Interestingly, excess noise is negatively correlated with the microwave reflection coefficient $|S_{11}|^2$ (Fig. 2c). Qualitatively, this correlation reflects the fact that noise generated by the sample can only be efficiently measured when the sample is impedance matched, $S_{11} = 0$. Note,

however, that S_{11} is weakly temperature dependent below 0.5 K, so that the temperature dependence in Fig. 2b should be attributed to a change in radiation, rather than a change in matching. More quantitatively, this observation leads us to propose a simple interpretation of the excess noise as arising from a device with an effective temperature T_s which is generally not equal to the cryostat temperature T_{cryo} . This model predicts a linear relationship between P and $|S_{11}|^2$

$$P/k_B = -\alpha|S_{11}|^2 (T_s - T_{\text{cryo}}) + T_s, \quad (1)$$

where α accounts for the net loss of the input lines and measurement chain, $\alpha|S_{11}|^2$ is the sample-referred reflection coefficient, and $\alpha|S_{11}|^2 = 1$ corresponds to complete reflection. Although S_{11} and α are generally frequency dependent, we measure in a narrow band such that S_{11} is constant, with negligible frequency dependence in α is expected.

To explore the noise model described above, we intentionally increase T_s by driving the sample out of equilibrium with a microwave tone far from our measurement band, measuring P and S_{11} for different drive strengths. In the absence of any drive, P and S_{11} are linearly related, consistent with the previously discussed correlations between noise power and microwave reflection (Fig. 3a). Under the application of a microwave drive at selected frequencies, P and $|S_{11}|^2$ maintain a linear relationship. Both the slope and vertical intercept increase with microwave drive power, while the intersection between curves is approximately drive-power independent. These observations have a straightforward interpretation within the noise model of Eq. 1. Both increasing vertical intercept and slope reflect an elevated sample temperature T_s , and a fixed crossing point at $-|S_{11}|^2 = 1/\alpha$ and $P/k_B = T_{\text{cryo}}$ reflects a constant T_{cryo} .

More formally, the best-fit slopes and vertical intercepts from Fig. 3a can be analyzed to extract α and the cryostat temperature T_{cryo} , as shown in Fig. 3b. The fit value of $\alpha = 64.5$ dB is compatible with an independent open-circuit calibration, and the fit value of $T_{\text{cryo}} = 50$ mK is self-consistent with the base cryostat temperature used in Fig. 2-4 to calculate P and T_s . We use this self-consistency criteria to define T_{cryo} . As a point of comparison, fixing α to the open-circuit calibration value of 63.9 dB yields a best-fit T_{cryo} of 28 mK. The linear relationship between P and $|S_{11}|^2$ and the compatibility of α and T_{cryo} with independent measurements gives evidence that Eq. 1 constitutes a predictive noise model for the device under study.

Using Eq. 1 and our calculated α and T_{cryo} , it is possible to make an inference of sample temperature from a microwave power spectral density (P) measurement. In the case of the anomalous metallic curve from Fig. 1b at -8.38 V, we find $T_s = 148$ mK, well above the base cryostat temperature determined either from the fits in Fig. 3a, by open circuit calibration, or by readings of the RuO_x thermometer installed on the mixing chamber plate. This temperature coincides with the onset of

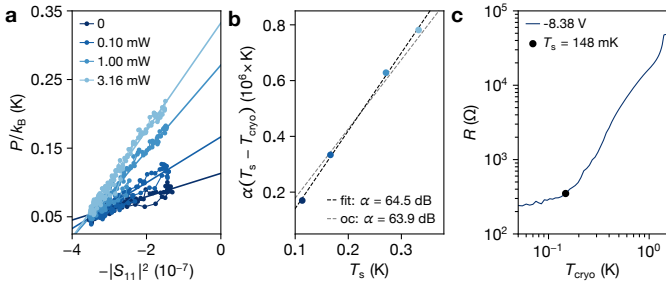


FIG. 3. **a**, Parametric plot of microwave power spectral density P vs microwave reflection $|S_{11}|^2$, both measured as a function of gate voltage. Power of microwave drive tone (at 547 MHz) at room temperature is indicated in legend; there is nominally 91 dB of attenuation between room temperature and the sample. A linear fit is performed to each curve to extract T_s and $\alpha(T_s - T_{\text{cryo}})$ according to Eq. 1. **b**, Slopes vs intercepts extracted from the fits to **a**. A subsequent linear fit (black) yields the net loss $\alpha = 64.5$ dB, and the cryostat temperature $T_{\text{cryo}} = 50$ mK. The fit from the independent open circuit calibration ('oc', red) of 63.9 dB is also shown. Uncertainty is less than the marker size. **c**, Measured resistance as a function of cryostat temperature is shown for the trace at -8.38 V from Fig. 1b, displaying anomalous metallic resistance saturation. T_s as calculated from Eq. 1 using α , T_{cryo} from the fits is plotted on the resistance curve. Resistance saturation begins approximately at this temperature.

anomalous metallic behavior, as shown in Fig. 3d. Thus, the anomalous metallic behavior can be understood as a consequence of the sample falling out of equilibrium with the cryostat below ≈ 150 mK. To verify that this phenomenon is generic, we have checked that metallic resistance saturation occurring at the calculated T_s as a function of cryostat temperature is observed when a microwave or low frequency heating tone is applied (see Supplement). In a different measurement configuration, we have also studied a sample which showed a higher-temperature onset of anomalous metallic behavior, and found that it emits more radiative noise (see Supplement), again consistent with a non-equilibrium origin of resistance saturation.

Summarizing up to this point, a simple model of non-equilibrium sample temperature explains the excess noise observed at the SIT, the correlated structure between P and $|S_{11}|^2$, and the origin of anomalous metallic behavior in our device. The nature of the non-equilibrium steady-state, however, has not yet been thoroughly explored. In ordinary metals, non-equilibrium steady states driven by an applied bias carry signatures of carrier charges and their interactions [27]. Near the superconductor-insulator transition, it has been put forward that current fluctuations about the non-equilibrium steady states are universally determined by the dynamical critical exponent [3, 4].

To explore this intriguing concept, we have studied the behavior of our device as a function of applied bias near the superconductor-insulator transition critical

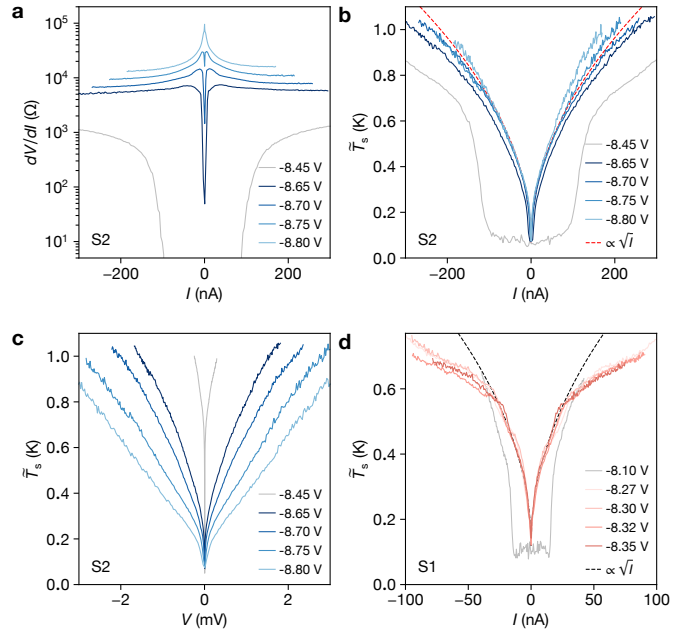


FIG. 4. **a**, Differential resistance dV/dI as a function of DC current, I , for different gate voltages (indicated by colors). Signatures of superconducting through insulating behavior are shown. **b**, Inferred sample temperature \tilde{T}_s as a function of measured DC current. Curves near criticality collapse onto one another. \sqrt{I} scaling shown, motivated by predictions [2–4]. **c**, Inferred \tilde{T}_s as a function of measured DC voltage, V . Curves do not collapse onto each other. **d**, Inferred \tilde{T}_s as a function of measured current in a second sample. Curves near criticality collapse onto one another. \sqrt{I} scaling shown, motivated by predictions [3, 4]. Panels **a** - **c** show data from device S2. Panel **d** shows data from device S1.

point. On the superconducting side of the SIT, resistance versus current I exhibits a pronounced zero-bias dip, whereas on the insulating side it exhibits a pronounced zero-bias peak (Fig. 4a). Over the same gate voltage and bias range, the non-equilibrium sample temperature \tilde{T}_s rises sharply with I . Here we have introduced \tilde{T}_s as an alternative inference of sample temperature in order to cancel out weak, time-dependent added noise drifts of the measurement chain (see Supplement). Expressing the total noise \tilde{T}_s in the units of current spectral density S_I , we estimate Fano factors F defined by $S_I = 2eFI$ [28] in the range 5 – 10, suggesting that heat does not leak and dissipate into the superconducting contacts [29]. Similar values were observed in earlier measurements of SNS junctions [30–32], which could microscopically arise from a combination of multiple Andreev reflections, Josephson radiation, or from the overheating of normal, diffusive regions between superconducting islands [33].

In contrast to resistance, whose zero-bias value varies by three orders of magnitude over the measured range of gate voltages, \tilde{T}_s is nearly gate voltage independent, and approximately collapses onto a single nonlinear curve

(Fig. 4b). The collapse only occurs when plotting \tilde{T}_s versus I ; other noise metrics such as the output noise power spectral density P or dependent variables such as voltage V do not exhibit a collapse (Fig. 4c). A qualitatively similar collapse is observed in a sample with a different geometry (Fig. 4d), confirming that it is a reproducible and geometry-independent phenomenon.

The observed scaling behavior of \tilde{T}_s is reminiscent of theoretical predictions of universal non-equilibrium behavior near the SIT [2–4]. These theories predict that current fluctuations are described by an effective temperature, mimicking the fluctuation-dissipation relation even though the system is profoundly non-equilibrium. Furthermore, the effective temperature is predicted to exhibit a universal scaling with applied bias, similar to the experimental data reported in Fig. 4. However, theories predict that the effective temperature scales as a function of applied voltage, in contrast to the experimentally observed scaling with current. It is unclear if this discrepancy is crucial, as these theories also predict a universal high-bias conductance linking current and voltage, while we observe a strong gate-dependent resistance [2, 34]. A full understanding of non-equilibrium responses near the SIT will require both further experimental work, for example varying sample sizes and model systems, as well

as further theoretical input. However, these initial results indicate the appealing possibility of universal, non-equilibrium behavior near quantum criticality.

We have introduced microwave radiometry as a powerful probe of behavior near the superconductor-insulator transition. We find that the origin of anomalous metallic behavior in our system is due to a failure to thermalize with the cryostat. This finding raises non-equilibrium behavior at the superconductor-insulator transition as an important topic for systematic study. As a first step in this direction, we have measured equivalent non-equilibrium temperatures as a function of applied bias, discovering scaling behavior that was anticipated based on Keldysh, Boltzmann, and gravity-gauge duality approaches [2–4]. It would be interesting to perform further thermometry measurements in a wider variety of model systems. A possible scenario is that anomalous metallic behavior is due to poor thermalization only in some cases, with genuine metallic behavior as $T \rightarrow 0$ occurring in others [1, 35–37]. The experimental approach demonstrated here, combined with recently-demonstrated on-chip bolometry [38], sets the stage for a new exploration of non-equilibrium behavior in Josephson arrays, weak superconductors, and other near-critical systems.

[1] A. Kapitulnik, S. A. Kivelson, and B. Spivak, Colloquium: Anomalous metals: Failed superconductors, *Rev. Mod. Phys.* **91**, 011002 (2019).

[2] D. Dalidovich and P. Phillips, Nonlinear transport near a quantum phase transition in two dimensions, *Phys. Rev. Lett.* **93**, 027004 (2004).

[3] A. G. Green, J. E. Moore, S. L. Sondhi, and A. Vishwanath, Current noise in the vicinity of the 2d superconductor-insulator quantum critical point, *Phys. Rev. Lett.* **97**, 227003 (2006).

[4] J. Sonner and A. G. Green, Hawking radiation and nonequilibrium quantum critical current noise, *Phys. Rev. Lett.* **109**, 091601 (2012).

[5] H. M. Jaeger, D. B. Haviland, B. G. Orr, and A. M. Goldman, Onset of superconductivity in ultrathin granular metal films, *Phys. Rev. B* **40**, 182 (1989).

[6] D. Ephron, A. Yazdani, A. Kapitulnik, and M. R. Beasley, Observation of quantum dissipation in the vortex state of a highly disordered superconducting thin film, *Phys. Rev. Lett.* **76**, 1529 (1996).

[7] O. Crauste, C. A. Marrache-Kikuchi, L. Bergé, D. Stanescu, and L. Dumoulin, Thickness dependence of the superconductivity in thin disordered nbsi films, *Journal of Physics: Conference Series* **150**, 042019 (2009).

[8] S. Eley, S. Gopalakrishnan, P. M. Goldbart, and N. Mason, Approaching zero-temperature metallic states in mesoscopic superconductor-normal-superconductor arrays, *Nature Physics* **8**, 59 (2012).

[9] Z. Han, A. Allain, H. Arjmandi-Tash, K. Tikhonov, M. Feigel'man, B. Sacépé, and V. Bouchiat, Collapse of superconductivity in a hybrid tin-graphene josephson junction array, *Nature Physics* **10**, 380 (2014).

[10] C. G. L. Böttcher, F. Nichele, M. Kjaergaard, H. J. Suominen, J. Shabani, C. J. Palmstrøm, and C. M. Marcus, Superconducting, insulating and anomalous metallic regimes in a gated two-dimensional semiconductor-superconductor array, *Nature Physics* **14**, 1138 (2018).

[11] C. G. L. Böttcher, F. Nichele, J. Shabani, C. J. Palmstrøm, and C. M. Marcus, Dynamical vortex transitions in a gate-tunable two-dimensional josephson junction array, *Phys. Rev. B* **108**, 134517 (2023).

[12] K. Ienaga, Y. Tamoto, M. Yoda, Y. Yoshimura, T. Ishigami, and S. Okuma, Broadened quantum critical ground state in a disordered superconducting thin film, *Nature Communications* **15**, 2388 (2024).

[13] I. Tamir, A. Benyamin, E. J. Telford, F. Gorniacyk, A. Doron, T. Levinson, D. Wang, F. Gay, B. Sacépé, J. Hone, K. Watanabe, T. Taniguchi, C. R. Dean, A. N. Pasupathy, and D. Shashar, Sensitivity of the superconducting state in thin films, *Science Advances* **5**, eaau3826 (2019), <https://www.science.org/doi/pdf/10.1126/sciadv.aau3826>.

[14] J. Shin, S. Park, and E. Kim, Effect of external electromagnetic radiation on the anomalous metallic behavior in superconducting ta thin films, *Phys. Rev. B* **102**, 184501 (2020).

[15] T. Mithun, Y. Kati, C. Danieli, and S. Flach, Weakly nonergodic dynamics in the gross-pitaevskii lattice, *Phys. Rev. Lett.* **120**, 184101 (2018).

[16] T. Mithun, C. Danieli, Y. Kati, and S. Flach, Dynamical glass and ergodization times in classical josephson junction chains, *Phys. Rev. Lett.* **122**, 054102 (2019).

[17] M. Pino, L. B. Ioffe, and B. L. Altshuler, Non-ergodic metallic and insulating phases of joseph-

son junction chains, *Proceedings of the National Academy of Sciences* **113**, 536 (2016), <https://www.pnas.org/doi/pdf/10.1073/pnas.1520033113>.

[18] M. Pino, V. E. Kravtsov, B. L. Altshuler, and L. B. Ioffe, Multifractal metal in a disordered josephson junctions array, *Phys. Rev. B* **96**, 214205 (2017).

[19] R. H. Dicke, R. Beringer, R. L. Kyhl, and A. B. Vane, Atmospheric absorption measurements with a microwave radiometer, *Phys. Rev.* **70**, 340 (1946).

[20] M. A. Castellanos-Beltran, K. D. Irwin, G. C. Hilton, L. R. Vale, and K. W. Lehnert, Amplification and squeezing of quantum noise with a tunable josephson metamaterial, *Nature Physics* **4**, 929 (2008).

[21] B. M. Brubaker, L. Zhong, Y. V. Gurevich, S. B. Cahn, S. K. Lamoreaux, M. Simanovskia, J. R. Root, S. M. Lewis, S. Al Kenany, K. M. Backes, I. Urdinaran, N. M. Rapidis, T. M. Shokair, K. A. van Bibber, D. A. Palken, M. Malnou, W. F. Kindel, M. A. Anil, K. W. Lehnert, and G. Carosi, First results from a microwave cavity axion search at 24 μ eV, *Phys. Rev. Lett.* **118**, 061302 (2017).

[22] J. Shabani, M. Kjaergaard, H. J. Suominen, Y. Kim, F. Nichele, K. Pakrouski, T. Stankevici, R. M. Lutchyn, P. Krogstrup, R. Feidenhans'l, S. Kraemer, C. Nayak, M. Troyer, C. M. Marcus, and C. J. Palmstrøm, Two-dimensional epitaxial superconductor-semiconductor heterostructures: A platform for topological superconducting networks, *Phys. Rev. B* **93**, 155402 (2016).

[23] W. Mayer, J. Yuan, K. S. Wickramasinghe, T. Nguyen, M. C. Dartailh, and J. Shabani, Superconducting proximity effect in epitaxial Al-InAs heterostructures, *Applied Physics Letters* **114**, 103104 (2019), https://pubs.aip.org/aip/apl/article-pdf/doi/10.1063/1.5067363/19772789/103104_1_online.pdf.

[24] M.-C. Cha, M. P. A. Fisher, S. M. Girvin, M. Wallin, and A. P. Young, Universal conductivity of two-dimensional films at the superconductor-insulator transition, *Phys. Rev. B* **44**, 6883 (1991).

[25] M. Swanson, Y. L. Loh, M. Randeria, and N. Trivedi, Dynamical conductivity across the disorder-tuned superconductor-insulator transition, *Phys. Rev. X* **4**, 021007 (2014).

[26] D. B. Haviland, Y. Liu, and A. M. Goldman, Onset of superconductivity in the two-dimensional limit, *Phys. Rev. Lett.* **62**, 2180 (1989).

[27] A. H. Steinbach, J. M. Martinis, and M. H. Devoret, Observation of hot-electron shot noise in a metallic resistor, *Phys. Rev. Lett.* **76**, 3806 (1996).

[28] Y. Blanter and M. Büttiker, Shot noise in mesoscopic conductors, *Physics Reports* **336**, 1 (2000).

[29] A. Denisov, A. Bubis, S. Piatrusha, N. Titova, A. Nasibulin, J. Becker, J. Treu, D. Ruhstorfer, G. Koblmüller, E. Tikhonov, and V. Khrapai, Heat-mode excitation in a proximity superconductor, *Nanomaterials* **12**, 10.3390/nano12091461 (2022).

[30] P. Dieleman, H. G. Bakkem, T. M. Klapwijk, M. Schicke, and K. H. Gundlach, Observation of andreev reflection enhanced shot noise, *Phys. Rev. Lett.* **79**, 3486 (1997).

[31] Y. Ronen, Y. Cohen, J.-H. Kang, A. Haim, M.-T. Rieder, M. Heiblum, D. Mahalu, and H. Shtrikman, Charge of a quasiparticle in a superconductor, *Proceedings of the National Academy of Sciences* **113**, 1743 (2016), <https://www.pnas.org/doi/pdf/10.1073/pnas.1515173113>.

[32] T. Hoss, C. Strunk, T. Nussbaumer, R. Huber, U. Staufer, and C. Schönenberger, Multiple andreev reflection and giant excess noise in diffusive superconductor/normal-metal/superconductor junctions, *Phys. Rev. B* **62**, 4079 (2000).

[33] H. Courtois, M. Meschke, J. T. Peltonen, and J. P. Pekola, Origin of hysteresis in a proximity josephson junction, *Phys. Rev. Lett.* **101**, 067002 (2008).

[34] A. G. Green and S. L. Sondhi, Nonlinear quantum critical transport and the schwinger mechanism for a superfluid-mott-insulator transition of bosons, *Phys. Rev. Lett.* **95**, 267001 (2005).

[35] M. Feigel'man and A. Larkin, Quantum superconductor–metal transition in a 2d proximity-coupled array, *Chemical Physics* **235**, 107 (1998).

[36] B. Spivak, A. Zyuzin, and M. Hruska, Quantum superconductor-metal transition, *Phys. Rev. B* **64**, 132502 (2001).

[37] B. Spivak, P. Oretto, and S. A. Kivelson, Theory of quantum metal to superconductor transitions in highly conducting systems, *Phys. Rev. B* **77**, 214523 (2008).

[38] B. Karimi, G. O. Steffensen, A. P. Higginbotham, C. M. Marcus, A. Levy Yeyati, and J. P. Pekola, Bolometric detection of josephson radiation, *Nature Nanotechnology* **10**, 1038/s41565-024-01770-7 (2024).

[39] A. J. Rimberg, T. R. Ho, i. m. c. Kurdak, J. Clarke, K. L. Campman, and A. C. Gossard, Dissipation-driven superconductor-insulator transition in a two-dimensional josephson-junction array, *Phys. Rev. Lett.* **78**, 2632 (1997).

[40] A. Goldman, Superconductor–insulator transitions in the two-dimensional limit, *Physica E: Low-dimensional Systems and Nanostructures* **18**, 1 (2003), 23rd International Conference on Low Temperature Physics (LT23).

[41] N. P. Breznay, M. A. Steiner, S. A. Kivelson, and A. Kapitulnik, Self-duality and a hall-insulator phase near the superconductor-to-insulator transition in indium-oxide films, *Proceedings of the National Academy of Sciences* **113**, 280 (2016), <https://www.pnas.org/doi/pdf/10.1073/pnas.1522435113>.

[42] N. P. Breznay and A. Kapitulnik, Particle-hole symmetry reveals failed superconductivity in the metallic phase of two-dimensional superconducting films, *Science Advances* **3**, e1700612 (2017).